

Supplementary Figures

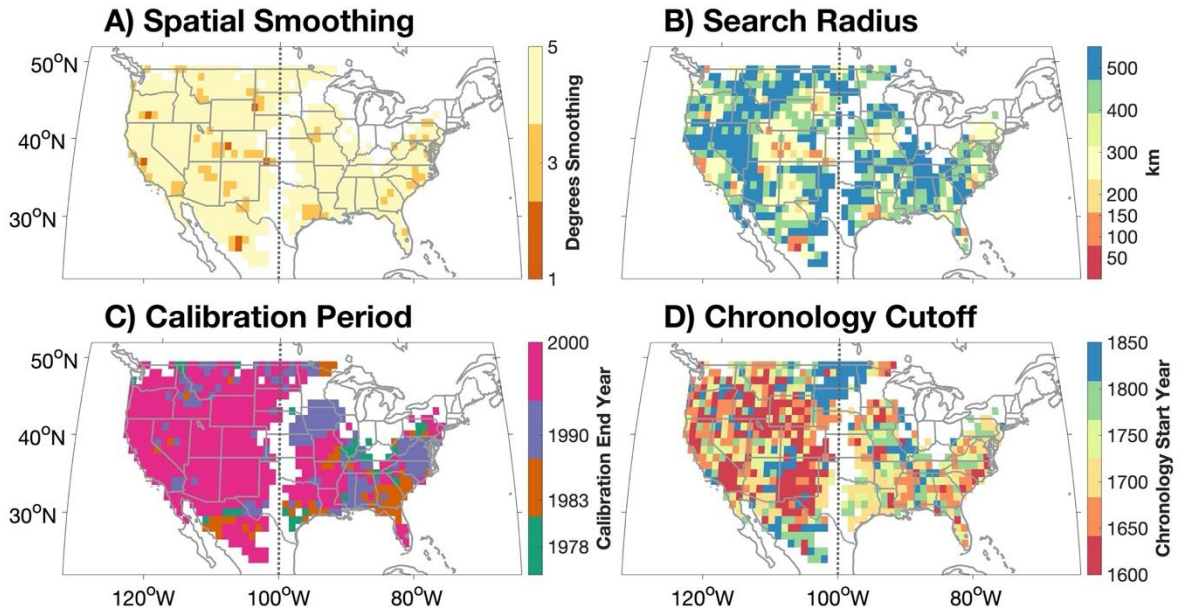


Figure S1. Maps of the (a) degree of target-dataset spatial smoothing, (b) search radius, (c) calibration period (starting in 1901), and (d) latest chronology start year used for final reconstruction of summer standardized soil moisture.

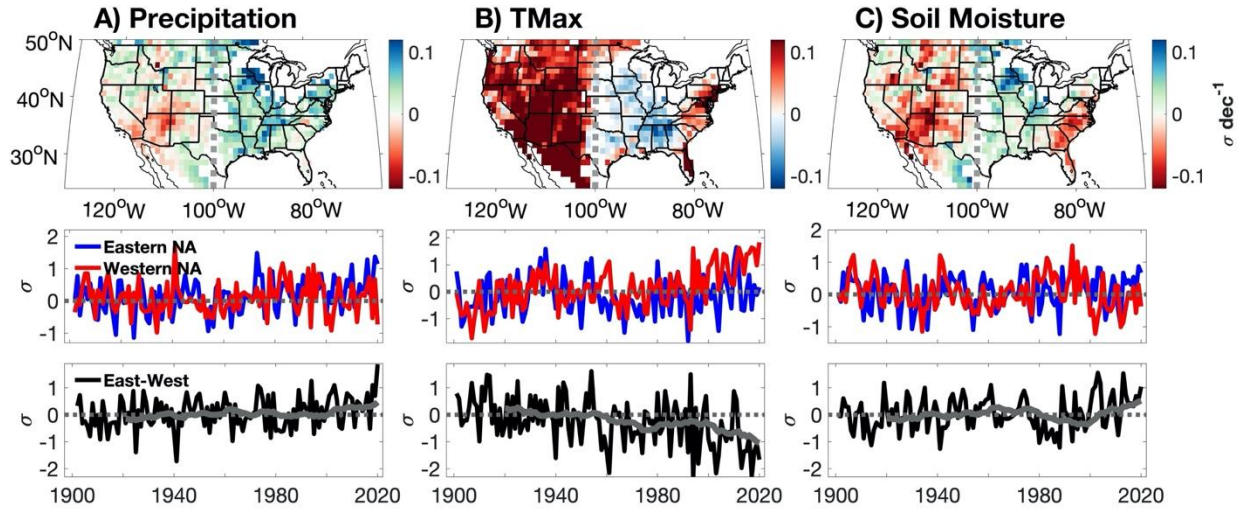


Figure S2. Same as Figure 1, but with grid cells *excluded* where soil moisture reconstruction $R^2 < 0.2$ or reconstruction does not extend to 1400 CE.

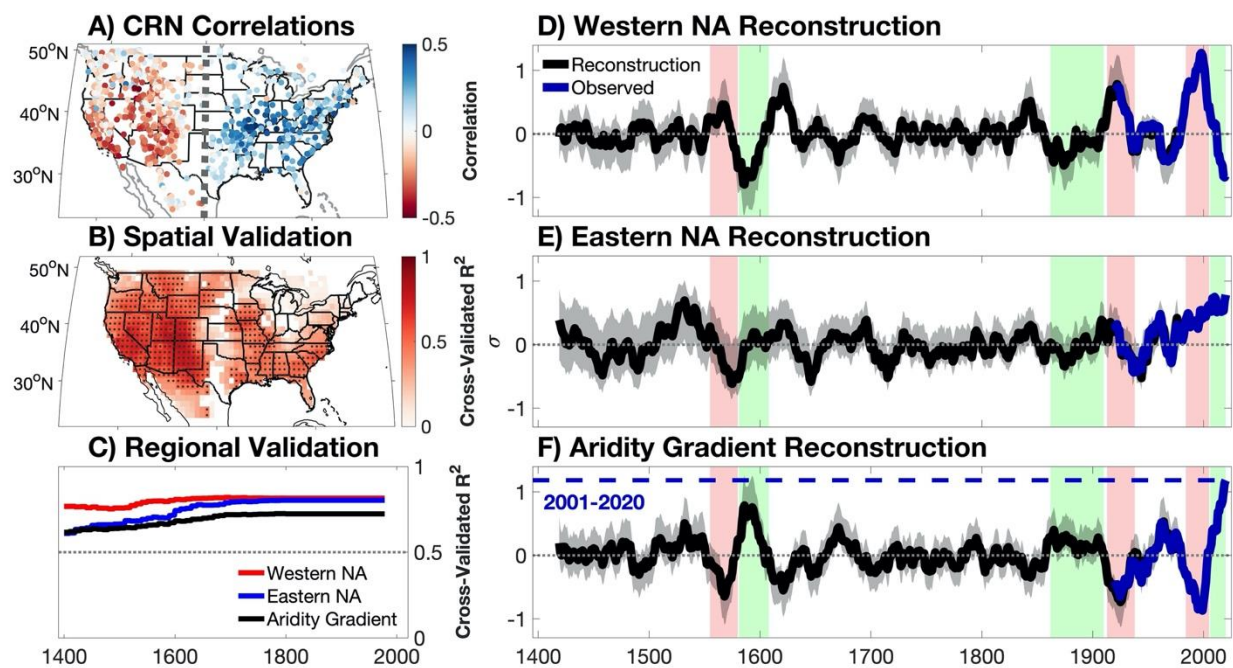


Figure S3. Same as Figure 2, but with grid cells *included* in the reconstruction where soil moisture reconstruction $R^2 < 0.2$.

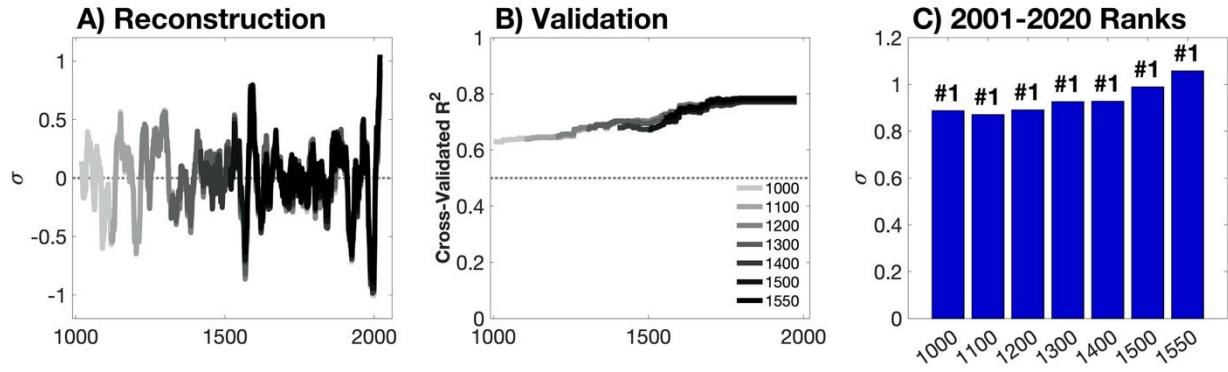


Figure S4. Comparison of reconstructions of varying lengths. (a) 20-year running-mean aridity gradient reconstructions for 7 alternate reconstructions (1000-, 1100-, 1200-, 1300-, 1400-, 1500-, and 1550-1978); (b) times series of cross-validated R^2 between observed aridity gradient and alternative reconstructions of aridity gradient; (c) magnitude of aridity gradient anomaly during 2001-2020 and the ranking of this anomaly relative to the most positive 20-year aridity gradient since 1000 CE.